Macromolecules
ARTICLE

Macromolecules **2009**, *42*, 4809–4816 **4809**
DOI: 10.1021/ma900713e

Polymerized Ionic Liquids: The Effect of Random Copolymer Composition on Ion Conduction

Hong Chen,[†] Jae-Hong Choi,[‡] David Salas-de la Cruz,[§] Karen I. Winey,[‡] and Yossef A. Elabd[†,*]

[†]*Department of Chemical and Biological Engineering, Drexel University, Philadelphia, Pennsylvania 19104,* [‡]*Department of Materials Science and Engineering, University of Pennsylvania, Philadelphia, Pennsylvania 19104, and* [§]*Department of Chemical and Biomolecular Engineering, University of Pennsylvania, Philadelphia, Pennsylvania 19104*

Received April 2, 2009; Revised Manuscript Received April 20, 2009

ABSTRACT: Ionic conductivity in new polymerized ionic liquids is of great interest as it applies to solid-state electrolytes for electrochemical and electromechanical applications. In this study, an ionic liquid monomer was synthesized and polymerized into random copolymers and their ionic conductivity and structure were investigated as a function of copolymer composition. Both nonionic−ionic and ionic−ionic copolymers were synthesized, where the nonionic and ionic monomers were hexyl methacrylate (HMA) and a methacrylate-based imidizolium neutralized with tetrafluoroborate (BF_4) or bis(trifluoromethane sulfonyl) imide (TFSI). In the nonionic−ionic copolymer, the ionic conductivity increased by over an order of magnitude with increasing HMA composition, even though the overall charge content decreased, because the addition of HMA significantly lowered the glass transition temperature. The ionic conductivity also increased by more than an order of magnitude in the ionic−ionic copolymer with increasing TFSI content, even though there was no change in the overall charge content, because substituting the larger anion TFSI for BF_4 resulted in weaker ionic interactions and also significantly lowered the glass transition temperature. In both types of copolymers, the temperature dependence of the ionic conductivity was well described by both Arrhenius and Vogel−Tamman−Fulcher models. An important difference between the two classes of random copolymers was that the nonionic−ionic copolymer exhibited microphase separation in X-ray scattering that correlated with a discontinuity in the increasing ionic conductivity with increasing HMA content suggesting that structure can also play a significant role in ion transport in polymerized ionic liquids.

Introduction

Solid-state polymer electrolytes with high ionic conductivities have been the subject of extensive research for applications in electrochemical devices, in part, because of the shortcomings of liquid electrolytes (e.g., leakage, flammability, toxicity, stability).[1−5] They alleviate the safety and stability concerns, while offering other attractive properties, such as thin-film forming ability, flexibility, and transparency. Recently, polymer electrolytes that contain ionic liquids have attracted remarkable interest.[6−14] Ionic liquids are composed of organic cations and anions, which are weakly associated and offer a unique combination of physicochemical properties, such as negligible vapor pressure, nonflammability, high ionic conductivity, a wide electrochemical window, and good chemical and thermal stability.[6,7] The use of ionic liquids in polymers as electrolytes has mainly focused on the mixtures of well-known polymers with ionic liquids using strategies, such as doping polymers with ionic liquids,[8] solution casting ionic liquid/polymer solutions,[9−12] and *in situ* polymerization of vinyl monomers in ionic liquids.[13] These ionic liquid/polymer mixtures have recently been investigated in solar cells,[15] supercapacitors,[16] batteries,[17] and fuel cells,[18] to name a few. However, ionic liquid/polymer mixtures require a compatible binary system, of which the reliable prediction for compatibility is still under investigation. Also, leakage issues associated with liquid electrolytes may not be resolved with an ionic liquid/polymer mixture system.

*To whom correspondence should be addressed. Telephone: 215.895.0986. Fax: 215.895.5837. E-mail: elabd@drexel.edu.

Relatively fewer investigations have focused on developing polymerizable ionic liquids as solid-state polymer electrolytes.[19−23] Polymerized ionic liquids (or polymers synthesized by polymerizing ionic liquid monomers) integrate macromolecular structure with ionic liquid moieties (in either the side group or backbone). The properties of polymerized ionic liquids are strongly associated with both the polymer and ionic liquid structure, where the structure of the cation and anion (e.g., ion type and substitute groups on the cation) are known to determine the physicochemical properties of ionic liquids.[6,7] The effect of the ionic liquid moiety on polymer properties, such as ionic conductivity,[19−23] microwave absorption,[24] and carbon dioxide sorption,[25−27] have recently been investigated.

Surprisingly, there are few reports on the ionic conductivity of polymerized ionic liquids,[19−23] the property most significant as it applies to electrochemical and electromechanical applications. Ohno and co-workers[19,20,23] explored the effect of the length of the spacer between the polymer backbone and ionic liquid moiety and the effect of different anions on conductivity in imidazolium-containing polymerized ionic liquids. Increasing the length of the spacer expectantly increased the conductivity, however, changing the anion (doubling the size with similar chemistry) unexpectedly also increased conductivity. Doubling the anion size resulted in an increase in conductivity of approximately 2 orders of magnitude, which coincided with a 50 K suppression in the glass transition temperature.

Although the fundamentals of ion transport in ionic liquids are currently under investigation,[28,29] it is evident that there are a number of other criteria to consider in polymerized ionic liquids compared to ionic liquids and ionic liquid/polymer mixtures.

Published on Web 05/11/2009

Polymerized ionic liquids differ in that the organic cation or anion is restricted in mobility compared to its more mobile counterion, unlike the ionic liquid or ionic liquid/polymer mixture where both cation and anion are mobile. The former alleviates the leakage issues associated with liquid electrolytes (similar to other solid-state polymer electrolytes), but usually results in a lower ionic conductivity (by several orders of magnitude) when compared to the latter. However, there is still limited work on understanding ionic conductivity in polymerized ionic liquids, therefore future work with new polymerized ionic liquids may result in ionic conductivities comparable to current state-of-the-art polymer electrolytes. The work by Ohno and co-workers[23] suggest that there are a number of factors that may impact ionic conductivity in polymerized ionic liquids, such as polymer architecture, glass transition temperature, molecular weight, and the chemistry of the polymer and ionic liquid moiety. Therefore, investigations on the ionic conductivity of new polymerized ionic liquids are warranted.

In this study, polymerized ionic liquid random copolymers were synthesized and their ionic conductivity and structure (X-ray scattering) were investigated as a function of copolymer composition. The first copolymer consists of ionic and nonionic monomers, where the ionic monomer consists of a methacrylate with imidazolium pendant cations neutralized with tetrafluoroborate (BF_4) anions and the nonionic monomer consists of hexyl methacrylate (HMA). The comonomers have similar chemical structure with and without the ionic liquid moiety. The second copolymer consists of the same ionic unit as the first copolymer, but the counterion (BF_4) was exchanged with bis(trifluoromethane sulfonyl)imide (TFSI) to various extents to form an all-ionic random copolymer. Conductivity was measured in both copolymers as function of increasing nonionic (HMA) and different ionic (TFSI) composition to probe the effect of polymer chain mobility and structure on ionic conductivity without significantly changing the polymer chemistry.

Experimental Section

Materials. 2-Bromoethanol (95%), methacryloyl chloride (97%, contains 200 ppm stabilizer monomethyl ether hydroquinone), triethylamine (≥99.5%), 1-butylimidazole (98%), sodium tetrafluoroborate (98%), lithium bis(trifluoromethane sulfonyl) imide (LiTFSI, 97%), hexyl methacrylate (98%), azobisisobutyronitrile (AIBN, 97%), lithium bromide (LiBr, 99.995% metals basis), dichloromethane (ACS reagent, ≥99.5%, contains 50 ppm stabilizer amylene), acetonitrile (anhydrous, 99.8%), diethyl ether (anhydrous, ≥99.7%, contains 1 ppm inhibitor BHT), and dimethylformamide (DMF, ACS reagent, ≥99.8% and HPLC grade, ≥99.9%) were purchased from Aldrich and used as received. Ultrapure deionized, reverse osmosis (RO) water (resistivity ~ 16 MΩ cm) was used as appropriate.

Synthesis of Imidazolium Monomer. The imidazolium-containing monomer 1-[2-methacryloyloxy)ethyl]-3-butylimidazolium tetrafluoroborate (MEBIm−BF_4) was synthesized by the method shown in Scheme 1. To a 250-mL flask in an ice bath, 50 mL of dichloromethane and 7.09 mL (0.1 mol) of 2-bromoethanol were added and stirred for 10 min. Then a solution of 9.72 mL (0.1 mol) of methacryloyl chloride in 10 mL of dichloromethane was added dropwise by addition funnel. After stirring the mixture for 30 min, 13.9 mL of triethylamine in 10 mL of dichloromethane was added dropwise. The reaction mixture was stirred overnight at room temperature and then filtered. The filtrate was washed thoroughly with 100 mL of DI water three times. The organic layer was collected and was dried with anhydrous magnesium sulfate. The solvent in the mixture was removed by vacuum at room temperature, which yielded clear liquid 2-bromoethyl methacrylate (80% yield).

In the synthesis of imidazolium bromide monomer, a small amount of inhibitor 2,6-di-*tert*-butyl-4-methylphenol was added

Scheme 1. Synthesis of Imidazolium-Containing Monomer, MEBIm−BF_4

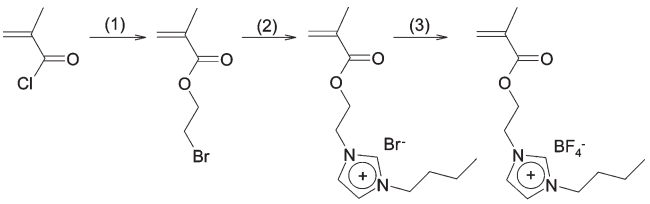

(1) 2-bromoethanol, triethylamine, dichloromethane, room temperature, 16 h

(2) 1-butylimidazole, 40 °C, 24 h

(3) $NaBF_4$, acetonitrile, room temperature, 48 h

to 13.51 g (0.07 mol) of 2-bromoethyl methacrylate and 8.69 g (0.07 mol) of 1-butyl imidazole. The mixture was stirred in a 40 °C water bath for 24 h and yielded a viscous liquid (100% yield). The liquid was dissolved in 40 mL of anhydrous acetonitrile. The solution was mixed with 11.1 g (0.1 mol) of $NaBF_4$ in 80 mL of anhydrous acetonitrile. The mixture was stirred for 48 h at room temperature and then filtered. The filtrate was dried under vacuum and the halide residue was removed by extensive water washing. Silver nitrate testing and elemental analysis confirmed that no halide was present in the monomer. The purified monomer was a slightly viscous clear liquid.

Anal. (Atlantic Microlab, Inc.) Found: C, 48.15; H, 6.56; N, 8.37; Br, 0; F, 19.67. ^{1}H NMR (UNITYINOVA 500 MHz, DMSO-d_6, ppm): 9.22 (s, 1H, N−CH−N), 7.80 (d, 2H, N−CH=CH−N), 6.01 (s, 1H, CH_2=C(CH_3)), 5.72 (s, 1H, CH_2=CH(CH_3)), 4.53 (t, 2H, N−CH_2−CH_2−O), 4.46 (t, 2H, N−CH_2−CH_2−O), 4.20 (t, 2H, N−CH_2−CH_2−CH_2−CH_3), 1.83 (s, 3H, CH_2=C(CH_3)), 1.78 (m, 2H, N−CH_2−CH_2−CH_2−CH_3), 1.21 (m, 2H, N−CH_2−CH_2−CH_2−CH_3), 0.88 (t, 3H, N−CH_2−CH_2−CH_2−CH_3).

Synthesis of Imidazolium Polymer. Imidazolium homopolymer poly(MEBIm−BF_4) was synthesized by a conventional free-radical polymerization. Inhibitors in the monomer were removed by washing in diethyl ether in an iced bath followed by drying under vacuum for 2 h in an iced bath. In a typical polymerization, imidazolium monomer (5 g), AIBN (5 mg), and DMF (5 g) were charged to a 20 mL glass vial. The vial was sealed with silicon rubber-lined open-top cap and purged with N_2 via needles for 30 min and then immersed in an oil bath at 60 °C for 12 h. After polymerization, the mixture was diluted with 5 g of DMF and was poured into cold methanol to precipitate the polymer. The polymer was washed with fresh methanol 3 times before drying under vacuum at 70 °C. ^{1}H NMR (UNITYINOVA 500 MHz, DMSO-d_6, ppm): 9.13 (1H, N−CH−N), 7.69−7.78 (2H, N−CH=CH−N), 4.19−4.46 (6H, N−CH_2−CH_2−O, N−CH_2−CH_2−CH_2), 1.78 (3H, CH_2−C(CH_3)), 1.27 (3H, N−CH_2−CH_2−CH_2−CH_3), 0.90 (4H, N−CH_2−CH_2−CH_2−CH_3), 0.43−0.67 (2H, CH_2−C(CH_3)).

Synthesis of Imidazolium Copolymers. Copolymers of the imidazolium polymer with hexyl methacrylate (HMA) were synthesized by the same free-radical polymerization using an appropriate amount of hexyl methacrylate and a total mass of monomer of 5 g. Copolymers with HMA at a comonomer fraction above 35 mol % were separated from the reaction system by precipitating in diethyl ether. They were purified by redissolving in an acetone/methanol cosolvent and reprecipitated in diethyl ether. The nonionic−ionic copolymer will be referred to as poly(HMA-*co*-MEBIm−BF_4) (60−70% yield).

Anion-exchange reaction of the homopolymer poly(MEBIm−BF_4) was conducted in acetonitrile at room temperature. Poly(MEBIm−BF_4) (0.5 g) and a desired amount of LiTFSI was dissolved in acetonitrile (10 mL) and stirred for 48 h. The product was precipitated out in deionized (DI) water and washed with DI water 3 times before drying under vacuum at

50 °C. The ionic−ionic copolymer will be referred to as poly (MEBIm−TFSI-*co*-MEBIm−BF_4).

Instruments. Molecular weight and polydispersity of poly (MEBIm−BF_4) was determined on a Waters GPC system equipped with a Styragel@HR 4 column, a 2410 RI detector, and a dual channel (λ = 254 and 270 nm) UV detector. Polymer was dissolved in HPLC grade DMF and 0.05 M of LiBr was added to reduce aggregation. Measurements were performed at a flow rate of 0.6 mL/min at 30 °C using polystyrene as standards. Thermal transitions were measured using DSC (TA Instruments, Q2000). Samples were sealed in a Tzero aluminum pan, cooled to −50 °C, and then heated to 300 at 10 °C/min under N_2 atmosphere. Thermal stabilities were measured with TGA (TA Instruments, Q50). Samples were put on an open platinum pan and heated at 10 °C/min under 50 mL/min N_2 flow. X-ray scattering was performed on the polymer cast films (100−200 μm in thickness) with the multiangle X-ray scattering system (MAXS), which consists of a Nonius FR591 rotating anode generator operated at 40 kV and 85 mA, an evacuated flight path, and a Bruker HiSTAR two-dimensional detector. Data were acquired at small, intermediate and wide angle regions for 5400, 3600, and 1200 s, respectively. Using Datasqueeze software,[30] the 2-D data were converted to 1-D data, intensity was corrected for primary beam intensity, and the corrected scattering from an empty cell was subtracted.

Ionic conductivity of the polymer films was measured between 10 Hz and 100 kHz using a Solartron AC impedance system (1260 impedance analyzer, 1287 electrochemical interface, Zplot software). Polymer films (100−200 μm in thickness) were prepared by solution casting on Teflon Petri dishes at ambient conditions in a fume food for 7 d. The films were then dried under vacuum at 60 °C for 8 h. For conductivity measurements, the polymer films were cut into 30 mm × 5 mm strips on a hot plate at a temperature above the polymer glass transition temperature and then stored in a desiccator until use. For conductivity measurements, the polymer films were assembled in a cell with four parallel electrodes and placed in an environmental chamber (Tenney) with controlled temperature (ranging from 30 to 150 °C) at a fixed relative humidity (below 10%). An alternating current was applied to the outer electrodes, while resistance was measured between the two inner electrodes. The real impedance or resistance (used to calculate ionic conductivity) was determined from the *x*-intercept of the imaginary versus real impedance data over a high frequency range. Polymer films were allowed to equilibrate at each temperature for 2 h and then measurements were taken every 15 min. Average resistance from 12 measurements was used to calculate conductivity using the equation $\sigma = L/(WTR)$, in which, σ is conductivity (S/cm), L is the distance between the two inner electrodes in the four-electrode cell (1 cm apart in this experiment), W and T are the width (cm) and thickness (cm) of the polymer film, respectively, and R is the resistance (Ω).

Results and Discussion

Imidazolium Monomer MEBIm−BF_4. The imidazolium monomer was synthesized by a three-step method as shown in Scheme 1. Imidazolium bromide monomer MEBIm−Br was a viscous liquid. It dissolved in water, DMF, DMSO, and acetonitrile. After exchanging the Br anion with BF_4 anion, it turned into a less viscous liquid. The resulting monomer MEBIm−BF_4 dissolved in DMF, DMSO, and acetonitrile, but was not water-soluble. Elemental analysis (error: 0.3 wt %) showed 0% halide residue in the final monomer. The reduced viscosity after anion exchange suggests a weaker association between the BF_4 anion and the imidazolium cation. Both monomers tend to autopolymerize at room temperature in a few days. Addition of inhibitor 2,6-di-*tert*-butyl-4-methylphenol and storage under 0 °C slows the autopolymerization to two weeks or longer. The reason for autopolymerization is not clear, but could be due to peroxide accumulation during exposure to air.[31]

Scheme 2. Structures of Imidazolium Copolymers

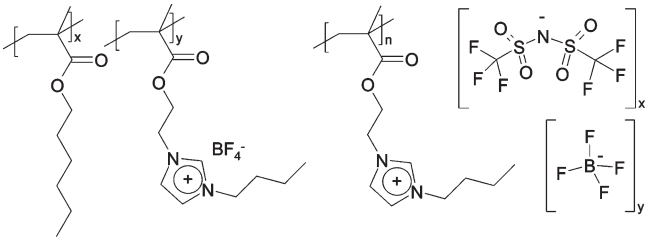

Synthesis of Imidazolium Copolymers. The imidazolium homopolymer poly(MEBIm−BF_4) was prepared by conventional free-radical polymerization in DMF using AIBN as the initiator. The conversion was 60−70% for ∼12-h reaction at 60 °C and the polymer was precipitated in methanol as a white solid. The structure was verified by ^{1}H NMR by the disappearance of the protons on the vinyl group (5.72 and 6.01 ppm). For the polymer synthesized at 0.1 wt % AIBN, the weight-average molecular weight determined by GPC in the presence of 0.05 M LiBr was 382 000 with a polydispersity of 1.27. The imidazolium polymer was hygroscopic and was only soluble in polar solvents such as DMF, DMSO, and acetonitrile. Polymer films prepared by solution casting from acetonitrile were transparent and brittle at ambient conditions.

The copolymers were synthesized with various concentrations of hexyl methacrylate by the same free-radical polymerization (structures shown in Scheme 2). Chemical structures were verified by ^{1}H NMR with peaks for HMA at 3.83 ppm (2H, O−CH_2−CH_2−CH_2) and 1.52 ppm (4H, O−CH_2−CH_2−CH_2). The other protons of HMA overlap with the structures of poly(MEBIm−BF_4) and change the intensity of the peaks. Concentrations of HMA in the copolymers were determined by measuring N content by elemental analysis. The copolymers with lower HMA content (e.g., ≤35 mol %) have similar solubility as the homopolymer poly(MEBIm−BF_4). At higher HMA content, the copolymers become partially soluble in DMF and start to form emulsion in less polar solvents, such as methanol and acetone. The copolymers also became more rubbery with the increase of HMA content. Copolymerization was allowed to proceed for 12 h and the conversion was similar to homopolymerization, i.e., 60−70%. At high conversions, the HMA composition in copolymers was higher than the composition in comonomers (Figure 1). This indicates that HMA has a higher tendency to homopolymerization than the imidazolium monomer MEBIm−BF_4.

In the anion-exchange of homopolymer poly(MEBIm−BF_4) with LiTFSI, the concentration of LiTFSI in the feed was varied to obtain various degrees of anion-exchange. Resulting polymers were regarded as copolymers of MEBIm−BF_4 and MEBIm−TFSI. To remove byproduct $LiBF_4$ and residue LiTFSI salt, the copolymers were extensively washed with DI water. The TFSI concentration was determined by measuring S content by elemental analysis. As shown in Figure 1, TFSI concentration in resulting polymers was nearly proportional to the feed concentration. No change was observed in solubility after anion-exchange. The copolymers with a TFSI mole fraction higher than 30 mol % became rubbery at ambient conditions and near 100 mol % TFSI the polymer became a very viscous liquid.

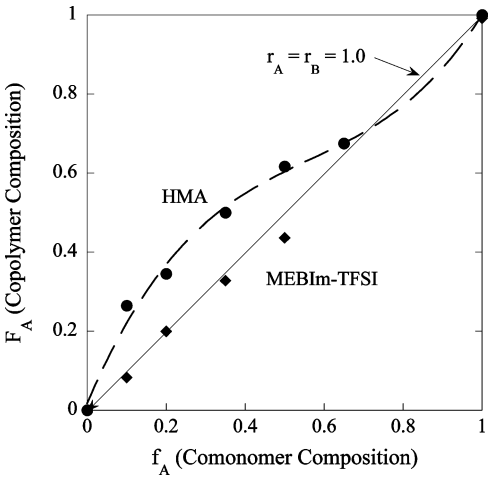

Figure 1. Comonomer composition (f_A) vs copolymer composition (F_A). Copolymer with HMA by copolymerization at high conversion (60−70%). Copolymers with MEBIm−TFSI by anion−exchange. Solid line represents $r_A = r_B = 1.0$ for comonomers in copolymerization at low conversion.

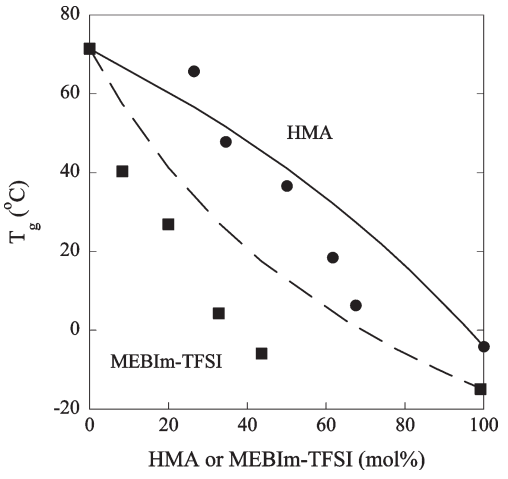

Figure 2. Glass transitions of imidazolium copolymers. Solid symbols are experimental data, where circles are poly(HMA-*co*-MEBIm−BF_4) and squares are poly(MEBIm−TFSI-*co*-MEBIm−BF_4). Lines are values calculated by Fox equation: solid line for poly(HMA-*co*-MEBIm−BF_4) and dashed line for poly(MEBIm−TFSI-*co*-MEBIm−BF_4).

Thermal Properties of Imidazolium Copolymers. Changes in the physical appearance (e.g., glassy to rubbery) of poly (MEBIm−BF_4) after copolymerization with HMA or anion-exchange with LiTFSI was observed, suggesting modified thermal behavior. DSC measurements were conducted to study the thermal transitions of the polymers. Over the temperature range of −50−300 °C, only a glass transition at 71.5 °C (midpoint method) was observed with homopolymer poly(MEBIm−BF_4), which suggests an amorphous structure. Copolymers with HMA also show glass transitions only. The glass transition temperature decreased significantly with increasing HMA concentration (Figure 2). The solid line in Figure 2 is the calculated T_g using the Fox equation for copolymers with random sequence distribution. At higher HMA content, deviation from this line was observed, which may suggest a morphology change in these compositions. At high conversion of copolymerization, sequence drift may occur and longer HMA segments dominate the polymer structure, suppressing the T_g of the copolymer to the HMA side. Compared to HMA copolymers, anion exchange of BF_4 anion with TFSI anion depresses the T_g more significantly. The T_gs also show a deviation from the Fox equation.

The thermal stability of the imidazolium polymers was investigated by TGA under N_2 atmosphere. Degradation temperatures (T_d) were measured at 5% loss in this study. Imidazolium homopolymer with BF_4 anion decomposes in one step above 322 °C (Figure 3a), which is higher than the T_d of methacrylic polymers (*e.g.*, T_d of poly(methyl methacrylate) is 272 °C[32]). Thermal decomposition of methacrylic polymers initiates from the backbone scission, which forms monomers.[32] The ionic group in imidazolium polymer may stabilize the backbone structure and make it more difficult to decompose under heat. It has been reported that imidazole is resistant to ring fission during thermal rearrangements of 1-alkyl- and 1-arylimidazoles at temperatures above 600 °C.[33,34] The homopolymer poly (HMA) was less thermally stable than poly(MEBIm−BF_4) evidenced by an onset decomposition temperature at 237 °C. Poly(HMA-*co*-MEBIm−BF_4) copolymers decompose in two steps with an onset temperatures close to 237 °C. The HMA component is responsible for the first step, while the second step can be attributed to imidazolium polymer component.

Replacing the BF_4 anion with near 100 mol % TFSI anion enhances the thermal stability by increasing the onset decomposition temperature to 373 °C (Figure 3b). The fully anion-exchanged polymer poly(MEBIm−TFSI) has a thermal decomposition behavior very similar to LiTFSI (curve not shown). The copolymers that contain both BF_4 and TFSI anions show thermal decomposition behavior of both homopolymers and an onset temperature similar to poly(MEBIm−BF_4). Enhancement of thermal stability with TFSI has been ascribed to the higher nucleophilicity of this ion.[34] The thermal stability suggests the potential use of imidazolium polymers in high-temperature electrochemical devices.

Ionic Conductivity. The temperature dependence of ionic conductivity (σ) was measured as a function of copolymer composition for both copolymers in this study. For the poly(HMA-*co*-MEBIm−BF_4) copolymers, the temperature dependence of ionic conductivity is shown in Figure 4a, where conductivity expectantly increases exponentially with increasing temperature from values on the order of 10^{-6} S/cm to values higher than 10^{-4} S/cm at 150 °C. Note that this is orders of magnitude lower than the ionic liquid, e.g., 0.36 S/cm at 25 °C for 1-butyl-3-methylimidazolium tetrafluoroborate (BMIm−BF_4).[35] We attribute this to the polymer structure that significantly limits the mobility of the ions. The imidazoluim cations are covalently attached to the polymer backbone that constrains motion and the BF_4 counteranions have reduced mobility due to the higher viscosity in the solid-state polymer film.

Interestingly, in Figure 4a, conductivity increases with increasing copolymer composition. In other words, increasing the composition of the nonionic HMA or reducing the overall charge content of the polymer actually increasing conductivity. This is seen more clearly in Figure 4b, where the ionic conductivity at 100 °C is plotted as a function of HMA composition. The conductivity increases slightly up to 50 mol % HMA and then abruptly increases by an order of magnitude at higher HMA compositions. It appears that the reduction in glass transition temperature (or increase in segmental motion of the polymer) with increasing copolymer HMA composition (see Figure 4b) has a more significant effect on ion mobility than the reduction in charge content, where one would expect a decrease in conductivity. The discontinuity in conductivity at higher copolymer

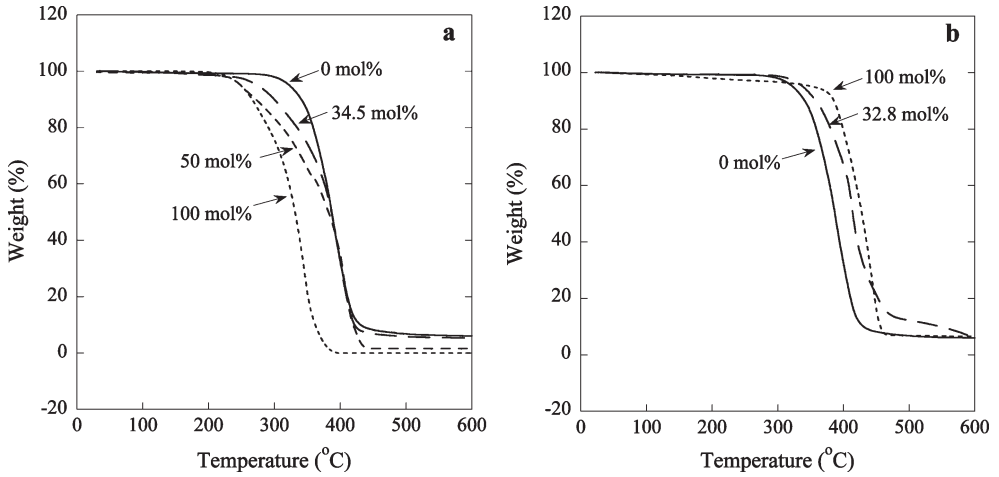

Figure 3. Thermal stability of imidazolium copolymers under N_2 atmosphere. (a) poly(HMA-*co*-MEBIm−BF_4) and (b) poly(MEBIm−TFSI-*co*-MEBIm−BF_4). Numbers represent mol % of copolymer HMA and MEBIm−TFSI determined by elemental analysis.

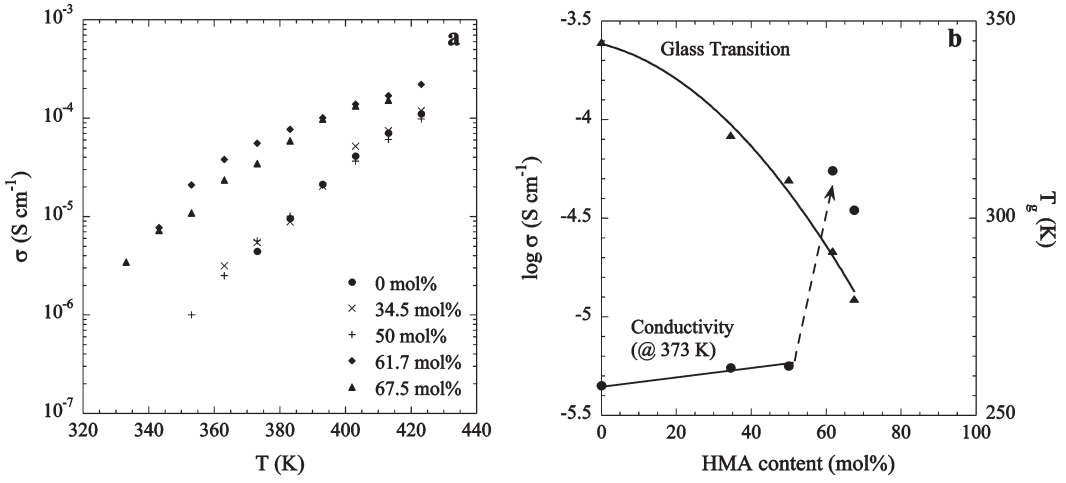

Figure 4. (a) Temperature and (b) composition and glass transition dependence of ionic conductivity for poly(HMA-*co*-MEBIm−BF_4). Numbers in part a correspond to mol % HMA and lines in part b correspond to trend lines.

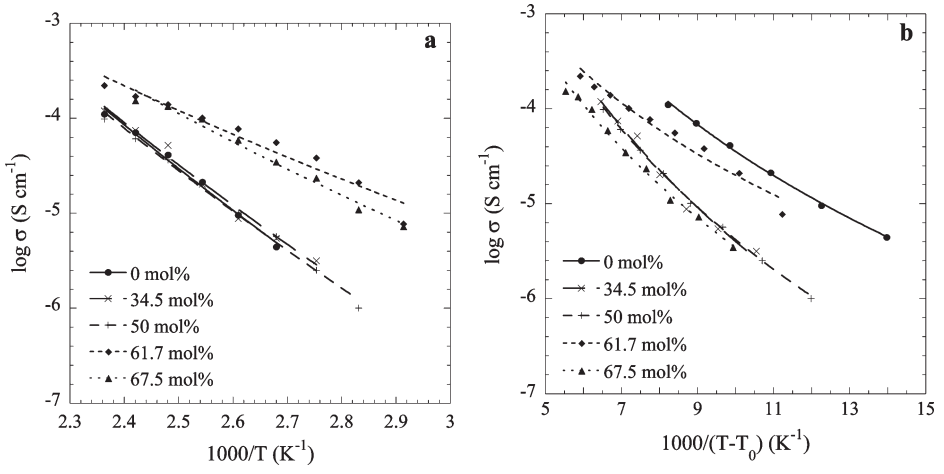

Figure 5. Temperature dependence of ionic conductivity for poly(HMA-*co*-MEBIm−BF_4): (a) regression to Ahrrhenius equation; (b) regression to VFT equation. Numbers on graphs correspond to mol % HMA.

compositions, however, may be the result of other factors (i.e., microphase-segregation).

Figure 5 shows a regression of the poly(HMA-*co*-MEBIm−BF_4) copolymer conductivity−temperature data to the Arrhenius equation, $\sigma = \sigma_0 \exp(E_a/RT)$, and the Vogel−Tamman−Fulcher (VFT) equation, $\sigma = \sigma_0 \exp[-B/(T - T_0)]$, where E_a (kJ/mol) is the activation energy and T_0 (K) is the temperature at which the polymer relaxation time becomes infinite or where the ion mobility goes to zero.[4,36] T_0 has been referred to as the equilibrium or true glass transition temperature and is usually approximately 50 K below the measured glass transition temperature.[4,36] The Arrhenius relation accounts for the thermal hopping frequency of ions, while the VFT model accounts for polymer relaxation or the segmental motion of the polymer

chains and has been related to the Cohen and Turbull free-volume theory.[37]

Parts a and b of Figure 5 show that the conductivity−temperature data for this copolymer appears to fit both the Arrhenius and VFT models reasonably well with minor deviations at higher HMA compositions (>60 mol %). Investigations on ionic liquid/polymer mixtures[13] and organic electrolytes[38] have shown deviations from the Arrhenius model as the experimental temperature approaches the glass transition temperature while the VFT equation fits a wider temperature range. In this study, the minimum temperature that conductivity was measured was at least 30 K above T_g. Others have suggested that when the experimental temperature exceeds T_0 sufficiently, then the Arrhenius and VFT models should merge.[4]

Table 1 lists the activation energies and equilibrium temperatures (T_0) determined for the regressions to the Arrhenius and VFT equations, respectively. As a function of HMA composition, the equilibrium temperatures ranged from 38 to 53 K below the measured glass transition temperature confirming a polymer relaxation limited process. With increasing HMA composition, the activation energy decreases slightly up to 50 mol % HMA and then abruptly decreases to almost half its value at compositions above 60 mol % HMA. The decrease in activation energy can be attributed to the reduction in glass transition temperature with increasing HMA content, where a medium with higher free volume imposes less resistance to ion mobility. The discontinuity in activation energy at higher HMA contents, however, parallels the discontinuity observed in conductivity at high HMA contents (Figure 4b). These discontinuities along with slight deviations to both the Arrhenius and VFT models at compositions >60 mol % HMA suggest other phenomena may be present at higher copolymer compositions.

Figure 6a shows the temperature dependence of ionic conductivity for the poly(MEBIm−TFSI-*co*-MEBIm−BF_4) copolymers at various copolymer compositions (up to 43.6 mol % TFSI). Similar to the poly(HMA-*co*-MEBIm−BF_4) copolymers, the conductivity at all compositions increases exponentially with increasing temperature. Unlike the poly(HMA-*co*-MEBIm−BF_4) copolymers, changing

Table 1. Activation Energies (Arrhenius), Equilibrium Temperatures (VFT), and Measured Glass Transition Temperatures for Poly(HMA-*co*-MEBIm−BF_4) Copolymers at Various Copolymer Compositions

copolymer (HMA, mol %)	E_a (kJ/mol)	T_0 (K)	T_g (K)
0	79.1	302	345
34.5	76.6	268	321
50.0	76.8	270	310
61.7	44.8	254	292
67.5	53.4	233	280

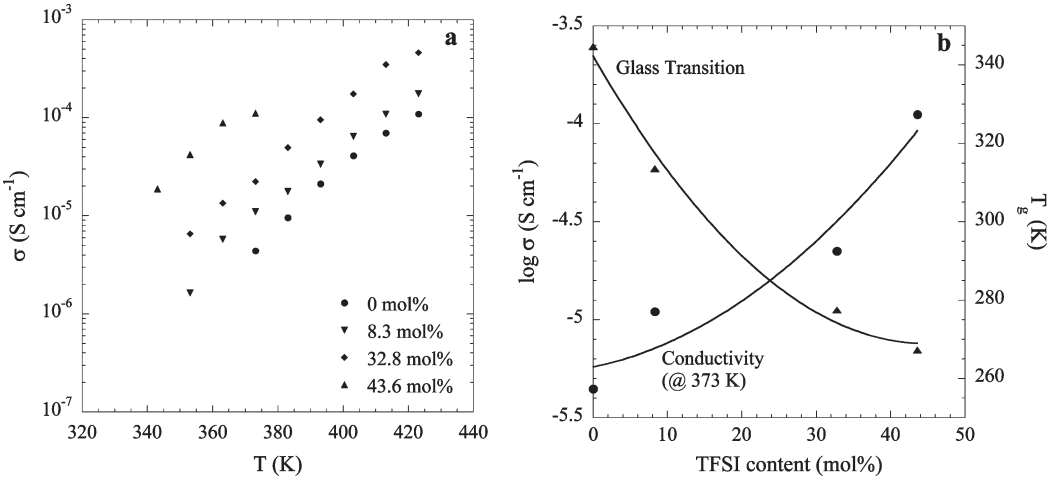

Figure 6. (a) Temperature and (b) composition and glass transition dependence of ionic conductivity for poly(MEBIm−TFSI-*co*-MEBIm−BF_4). Numbers in part a correspond to mol % TFSI, and lines in part b correspond to trend lines.

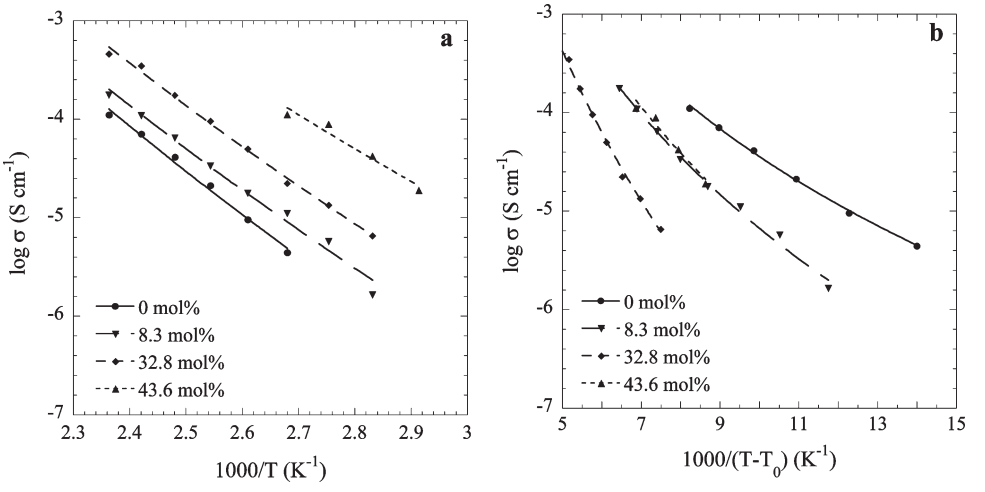

Figure 7. Temperature dependence of ionic conductivity for poly(MEBIm−TFSI-*co*-MEBIm−BF_4): (a) regression to Arrhenius equation; (b) regression to VFT equation. Numbers on graphs correspond to mol % TFSI.

copolymer composition for this copolymer merely corresponds to changing the ratio of anions (from BF_4 to TFSI anions) not a change in the imidazolium pendant group. In other words, changing copolymer composition has no effect on the overall charge content in this system. Interestingly, the conductivity increases with increasing TFSI content, even though the conductivity of the corresponding ionic liquids are similar (0.36 S/cm at 25 °C for BMIm−BF_4 and 0.38 S/cm at 25 °C for BMIm−TFSI).[35]

Figure 6b shows the conductivity at 373 K and the glass transition temperature as function of TFSI composition, where conductivity increases smoothly by over an order of magnitude with increasing TFSI composition. Similar to the HMA copolymers, it appears that the reduction in glass transition temperature has a significant effect on ion mobility, where one would predict no change in conductivity by merely changing the anion type for ionic liquids of the similar conductivity. Unlike the HMA copolymers, the increase in conductivity was continuous over the copolymer composition investigated.

Figure 7 shows a regression of the poly(MEBIm−TFSI-*co*-MEBIm−BF_4) copolymer conductivity−temperature data to the Arrhenius and VFT equations, where the data appears to fit reasonably well to both models over this temperature range. Again, the minimum temperature that conductivity was measured was at least 30 K above T_g. Table 2 lists the activation energies and equilibrium temperatures determined from the regressions to the Arrhenius and VFT equations, respectively. As a function of TFSI composition from 0 to 43 mol %, the equilibrium temperatures ranged from 40 to 58 K below the measured glass transition temperature confirming a polymer relaxation limited process. With increasing TFSI composition, the activation energy decreases from 79 to 67 kJ/mol. The decrease in activation energy can be attributed to the reduction in glass transition temperature with increasing TFSI content.

Table 2. Activation Energies (Arrhenius), Equilibrium Temperatures (VFT), and Measured Glass Transition Temperatures for Poly (MEBIm−TFSI-*co*-MEBIm−BF_4) Copolymers at Various Copolymer Compositions

copolymer (HMA, mol %)	E_a (kJ/mol)	T_0 (K)	T_g (K)
0	79.1	302	345
8.3	75.4	268	314
32.6	74.6	220	277
43.6	66.7	227	267

Morphology. To study the morphology of the imidazolium copolymers, X-ray scattering measurements were performed on the polymer films at room temperature. As shown in Figure 8, both types of copolymers exhibit peaks at 14.0 and 4.51 nm^{-1}, corresponding to the amorphous halo and local ordering of alkyl segments, respectively. Excess scattering and broad peaks appear at q = 0.8 to 3 nm^{-1} for poly(HMA-*co*-MEBIm−BF_4), while this q region in poly(MEBIm−TFSI-*co*-MEBIm−BF_4) is featureless. This suggests that the HMA copolymers are microphase separated or have significant concentration fluctuations wherein the nonionic monomeric units segregate from the ionic monomeric units. This local heterogeneity could be the origin of the discontinuities in ionic conductivity (Figure 4b) and activation energy (Table 1). In contrast, the X-ray scattering from poly(MEBIm−TFSI-*co*-MEBIm−BF_4) indicates a homogeneous, amorphous morphology that corresponds to a smoothly varying ionic conductivity and E_a. Thus, both the segmental motion and the morphology impact ion mobility. At lower angles (q < 0.7 nm^{-1}), the intensity approximately follows a q^{-3} dependence, which is independent of copolymer type or composition. The origin of this upturn is not the collimation of the system, because the scattering from an empty cell has been subtracted. Thus, although the copolymer films are transparent, we currently attribute the low angle scattering to microvoids.

Conclusions

In this study, an ionic liquid monomer was synthesized and polymerized to form nonionic−ionic and ionic−ionic random copolymers. These copolymers were studied to investigate the effect of copolymer composition on ionic conductivity and morphology. The polymerized ionic liquid homopolymer contained a methacrylate-based backbone with imidazolium cation side groups neutralized with mobile BF_4 anions. The nonionic−ionic copolymer was synthesized by copolymerization with hexyl methacrylate (HMA), while the ionic−ionic copolymer was synthesized by anion-exchange with LiTFSI. Therefore, the effect of nonionic moiety and anion type on ionic conductivity was explored with these two types of copolymers. With increasing

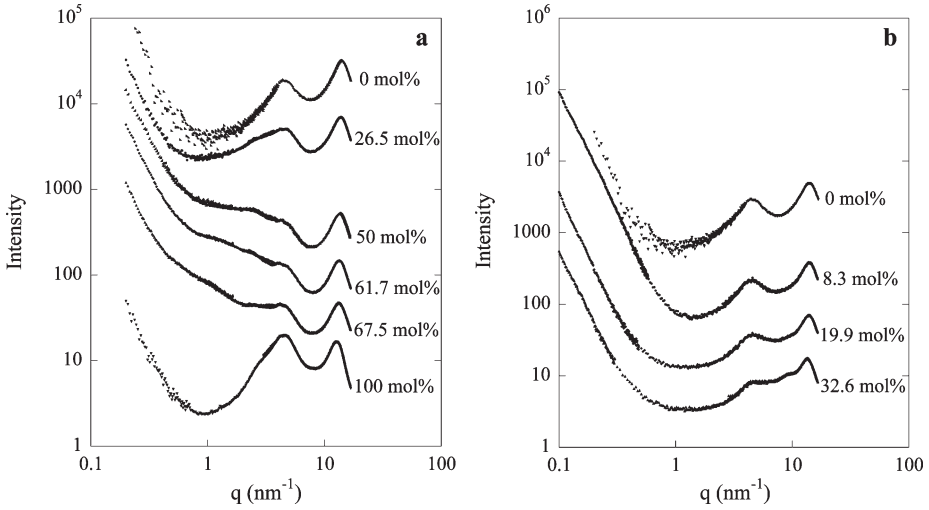

Figure 8. X-ray scattering intensities (a.u.) as a function of scattering vector for (a) poly(HMA-*co*-MEBIm−BF_4) and (b) poly(MEBIm−TFSI-*co*-MEBIm−BF_4). Numbers on graphs correspond to mol % HMA and MEBIm−TFSI, respectively. X-ray beam was normal to the plane of the polymer film. Graphs are displayed on a log−log scale to accommodate the wide range of scattering vector.

HMA and TFSI composition, the glass transition temperature, T_g, decreased significantly compared to the MEBImBF$_4$ homopolymer and the ionic conductivity increased by over an order of magnitude. In the HMA copolymer, the enhanced ionic conductivity at a lower ionic concentration shows that the reduced T_g has a more significant effect on ionic conductivity than the overall charge content. Similarly, increasing TFSI composition lowers the T_g because larger anions have weaker association with the cation and results in increased ionic conductivity. Over the temperature range of $\sim T_g$ + 30 to 423 K, the ionic conductivity of both nonionic−ionic and ionic−ionic copolymers increased with an increase in temperature and showed a reasonably good fit to both the Arrhenius and VFT equations. The equilibrium temperature, T_0, regressed from the VFT model was approximately 50 K below the measured T_g for both copolymers, confirming a polymer relaxation limited process for ion conduction. In addition, X-ray scattering revealed microphase segregation in the HMA copolymers that may account for discontinuous increase in ionic conductivity and activation energy. The ionic−ionic random copolymer showed no evidence of microphase separation and the ionic conductivity varied smoothly with composition. Thus, this study has demonstrated the importance of both the glass transition and morphology on ionic conductivity in polymerized ionic liquids.

Acknowledgment. The authors gratefully acknowledge assistance from Dr. Yuesheng Ye and Prof. Giuseppe R. Palmese with GPC measurements. This work is supported in part by the U.S. Army Research Office under Grant No. W911NF-07-1 0452 Ionic Liquids in Electro-Active Devices (ILEAD) MURI.

References and Notes

(1) Xu, K. *Chem. Rev.* **2004**, *104*, 4303.
(2) Gray, F. M. *Polymer Electrolytes*; RSC Materials Monographs; The Royal Society of Chemistry, Information Services: Letchworth, U.K., **1997**.
(3) Ratner, M. A.; Shriver, D. F. *Chem. Rev.* **1988**, *88*, 109.
(4) MacCallum, J. R., Vincent, C. A., Eds. *Polymer Electrolyte Reviews*; Elsevier Applied Science: London, **1987**.
(5) Gray, F. M.; MacCallum, J. R.; Vincent, C. A.; Giles, J. R. M. *Macromolecules* **1988**, *21*, 392.
(6) Brennecke, J. F.; Maginn, E. J. *AIChE J.* **2001**, *47*, 2384.
(7) Wasserscheid, P., Welton, T., Eds. *Ionic Liquids in Synthesis*; Wiley-VCH Verlag: Weinheim, Germany, **2003**.
(8) Doyle, M.; Choi, S. K.; Proulx, G. *J. Electrochem. Soc.* **2000**, *147*, 34.
(9) He, Y. Y.; Boswell, P. G.; Buhlmann, P.; Lodge, T. P. *J. Phys. Chem. B* **2007**, *111*, 4645.
(10) He, Y. Y.; Lodge, T. P. *Chem. Commum.* **2007**, *26*, 2732.
(11) Lewandowski, A.; Swiderska, A. *Solid State Ionics* **2004**, *169*, 21.
(12) Yeon, S. H.; Kim, K. S.; Choi, S.; Cha, J. H.; Lee, H. *J. Phys. Chem. B* **2005**, *109*, 17928.
(13) Susan, M.; Kaneko, T.; Noda, A. Watanabe, M. *J. Am. Chem. Soc.* **2005**, *127*, 4976.
(14) Ueki, T.; Watanabe, M. *Macromolecules* **2008**, *41*, 3739.
(15) Kawano, R.; Matsui, H.; Matsuyama, C.; Sato, A.; Susan, M. A. B. H.; Tanabe, N.; Watanabe, M. *J. Photochem. Photobiol., A* **2004**, *164*, 87.
(16) Lee, J; Panzer, M. J.; He, Y.; Lodge, T. P.; Frisbie, C. D. *Macromolecules*, **2007**, *129*, 4532.
(17) Shobukawa, H.; Tokuda, H.; Tabata, S. I.; Watanabe, M. *Electrochim. Acta* **2004**, *50*, 305.
(18) Noda, A.; Bin Hasan Susan, A.; Kudo, K.; Mitsushima, S.; Hayamizu, K.; Watanabe, M. *J. Phys. Chem. B* **2003**, *107*, 4024.
(19) Yoshizawa, M.; Ohno, H. *Electrochem. Acta* **2001**, *46*, 1723.
(20) Yoshizawa, M.; Ohno, H. *Chem. Lett.* **1999**, *28*, 889.
(21) Ohno, H.; Ito, K. *Chem. Lett.* **1998**, *27*, 751.
(22) Ohno, H.; Nakai, Y.; Ito, K. *Chem. Lett.* **1998**, *27*, 15.
(23) Matsumi, N.; Sugai, K.; Miyake, M.; Ohno, H. *Macromolecules* **2006**, *39*, 6924.
(24) Tang, J.; Radosz, M.; Shen, Y. *Macromolecules* **2008**, *41*, 493.
(25) Tang, J.; Tang, H.; Sun, W.; Radosz, M.; Shen, Y. *J. Polym. Sci., Part A: Polym. Chem.* **2005**, *43*, 5477.
(26) Tang, H.; Tang, J.; Ding, S.; Radosz, M.; Shen, Y. *J. Polym. Sci., Part A: Polym. Chem.* **2005**, *43*, 1432.
(27) Ding, S.; Tang, H.; Radosz, M.; Shen, Y. *J. Polym. Sci., Part A: Polym. Chem.* **2004**, *42*, 5749.
(28) Sangoro, J.; Iacob, C.; Serghei, A.; Naumov, S.; Galvosas, P.; Karger, J.; Wespe, C.; Bordusa, F.; Stoppa, A.; Hunger, J.; Buchner, R.; Kremer, F. *J. Chem. Phys.* **2008**, *128*, 214509.
(29) Sangoro, J.; Serghei, A.; Naumov, S.; Galvosas, P.; Karger, J.; Wespe, C.; Bordusa, F.; Kremer, F. *Phys. Rev. E* **2008**, *77*, 051202.
(30) Heiny, P. A. *Commum. Powder Diffr. Newslett.* **2005**, *32*, 9.
(31) Alaimo, R. J. *Handbook of Chemical Health and Safety*; Oxford University Press: New York, NY, **2001**.
(32) Grassie, N.; Scott, G. *Polymer Degradation and Stabilisation*; Cambridge University Press: Cambridge, U.K., **1985**.
(33) Ngo, H. L.; LeCompte, K.; Hargens, L.; McEwen, A. B. *Thermochim. Acta* **2000**, *357−358*, 97.
(34) Awad, W. H.; Gilman, J. W.; Nyden, M.; Harris, R. H., Jr.; Sutto, T. E.; Callahan, J.; Trulove, P. C.; Delong, H. C.; Fox, D. M. *Thermochim. Acta* **2004**, *409*, 3.
(35) Tokuda, H.; Tsuzuki, S.; Susan, M. A. B. H.; Hayamizu, K.; Watanabe, M. *J. Phys. Chem. B* **2006**, *110*, 19593.
(36) Vogel, H. *Phys. Z.* **1921**, *22*, 645. Tammann, G.; Hesse, W. *Z. Anorg. Allgem. Chem.* **1926**, *156*, 245. Fulcher, G. S. *J. Am. Ceram. Soc.* **1925**, *8*, 339.
(37) Cohen, M. H.; Turnbull, D. *J. Chem. Phys.* **1959**, *31*, 1164.
(38) Gu, G. Y.; Laura, R.; Abraham, K. M. *Electrochem. Solid. Lett.* **1999**, *2*, 486.